



## On the evolution of sub- and super-saturated water uptake of secondary organic aerosol in chamber experiments from mixed precursors

Yu Wang<sup>1,\*</sup>, Aristeidis Voliotis<sup>1</sup>, Dawei Hu<sup>1</sup>, Yunqi Shao<sup>1</sup>, Mao Du<sup>1</sup>, Ying Chen<sup>2</sup>, M. Rami Alfarra<sup>1,3,4</sup>,  
Gordon McFiggans<sup>1,\*</sup>

5 <sup>1</sup>Centre for Atmospheric Science, Department of Earth and Environmental Sciences, The University of  
Manchester, Manchester M13 9PL, UK

<sup>2</sup>Exeter Climate Systems, University of Exeter, Exeter, EX4 4QE, UK

<sup>3</sup>National Centre for Atmospheric Science, Department of Earth and Environmental Sciences, The  
University of Manchester, Manchester, M13 9PL, UK

10 <sup>4</sup>Environment & Sustainability Center, Qatar Environment & Energy Research Institute, Doha, Qatar

\*Correspondence to: Yu Wang ([yu.wang@manchester.ac.uk](mailto:yu.wang@manchester.ac.uk)); Gordon McFiggans  
([g.mcfiggans@manchester.ac.uk](mailto:g.mcfiggans@manchester.ac.uk))



## Abstract.

To better understand the chemical controls of sub- and super-saturated aerosol water uptake, we designed  
20 and conducted a series of chamber experiments to investigate the evolution of aerosol physicochemical  
properties during SOA formation from the photochemistry of single or mixed biogenic ( $\alpha$ -pinene,  
isoprene) and anthropogenic (*o*-cresol) volatile organic compounds (VOCs) in the presence of ammonium  
sulphate seeds. During the six-hour experiments, the cloud condensation nuclei (CCN) activity at super-  
saturation of water (0.1 ~ 0.5 %), hygroscopic growth factor at 90% RH, and non-refractory PM<sub>1</sub> chemical  
25 composition were recorded concurrently. The hygroscopicity parameter  $\kappa$  was used to represent water  
uptake ability below and above water saturation, and the  $\kappa$ -Köhler approach was implemented to predict  
the CCN activity from the sub-saturated hygroscopicity.

The sub- and super-saturated water uptake (in terms of  $\kappa_{\text{HTDMA}}$  and  $\kappa_{\text{CCN}}$ ) were mainly controlled by the  
SOA mass fraction which depended on the SOA production rate of the precursors, and the SOA  
30 composition played a second-order role. For the reconciliation of  $\kappa_{\text{HTDMA}}$  and  $\kappa_{\text{CCN}}$ , the  $\kappa_{\text{HTDMA}} / \kappa_{\text{CCN}}$   
ratio increased with the SOA mass fraction and this was observed in all investigated single and mixed  
VOC systems, independent of initial VOC concentrations and sources. For all VOC systems, the mean  
 $\kappa_{\text{HTDMA}}$  of aerosol particles was ~ 25 % lower than the  $\kappa_{\text{CCN}}$  at the beginning of the experiments with  
inorganic seeds. With the increase of condensed SOA on seed particles throughout the experiments, the  
35 discrepancy of  $\kappa_{\text{HTDMA}}$  and  $\kappa_{\text{CCN}}$  became weaker (down to ~ 0 %) and finally the mean  $\kappa_{\text{HTDMA}}$  was ~ 60  
% higher than  $\kappa_{\text{CCN}}$  on average when the SOA mass fraction approached ~ 0.8. This is possibly attributable  
to the non-ideality of solutes at different RH or the different co-condensation of condensable organic  
vapours within the two instruments. As a result, the predicted CCN number concentrations from the  
 $\kappa_{\text{HTDMA}}$  and particle number size distribution were ~ 10 % lower than CCN counter measurement on  
40 average at the beginning, and further even turned to an overestimation of ~ 20 % on average when the  
SOA mass fraction was ~ 0.8. This chemical composition-dependent performances of  $\kappa$ -Köhler approach  
on CCN prediction can introduce a variable uncertainty in predicting cloud droplet numbers from the sub-  
saturated water uptake.



## 1 Introduction

45 Aerosol-cloud interactions, that is how aerosol particles influence cloud formation, largely influence Earth radiation budget and the current climate projections (Boucher et al., 2013;Lohmann and Feichter, 2005;Bellouin et al., 2020). The reliability of cloud condensation nuclei (CCN) activity predicted from the aerosol hygroscopic growth under sub-saturated condition remains unresolved, e.g. (Cruz and Pandis, 1998;VanReken et al., 2005;Huff Hartz et al., 2005;Prenni et al., 2007;Petters et al., 2009;Wex et al., 50 2009;Ervens et al., 2007;Good et al., 2010b;Liu et al., 2018). One of the main knowledge gap is the precise determination of CCN activity involving complex organic aerosols. A large portion of organic aerosols are secondary organic aerosol (SOA) (Zhang et al., 2007;Jimenez et al., 2009), formed from oxidation of gaseous volatile organic compounds (VOCs) via gas-particle partitioning (Hallquist et al., 2009). Although the organic aerosol components are less soluble and consequently less hygroscopic than 55 the referenced inorganic compounds (e.g. sulphate, nitrate) (Sun and Ariya, 2006;Alfarra et al., 2013;McFiggans et al., 2006;Topping et al., 2013a;Kreidenweis and Asa-Awuku, 2014;Liu et al., 2018;Huff Hartz et al., 2005;King et al., 2009;Good et al., 2010b), they can play an important role in the cloud formation globally due to its ubiquitous large fraction (20 ~ 90 %) in fine particulate matter mass (Kanakidou et al., 2005;Jimenez et al., 2009;Zhang et al., 2007). Nevertheless, our understanding of its 60 hygroscopicity and CCN activity remains uncertain, due to the wide range of solubility, volatility and complex composition of organic compounds from different sources (Hallquist et al., 2009;Goldstein and Galbally, 2007;Shrivastava et al., 2017).

Previous laboratory reconciliation studies of aerosol hygroscopicity and CCN activity were mainly focused on experiments investigating the nucleation of SOA from single biogenic VOC oxidation e.g. 65 (Prenni et al., 2007;Wex et al., 2009;Petters et al., 2009;Alfarra et al., 2013;Liu et al., 2018;Zhao et al., 2016;Duplissy et al., 2008), from anthropogenic VOC (Zhao et al., 2016;Liu et al., 2018;Prenni et al., 2007) and a few from biogenic-anthropogenic VOC mixtures e.g. (Zhao et al., 2016). However, the findings are not consistent. For the biogenic SOA, most studies found that the single hygroscopicity parameter ( $\rho_{\text{ion}}$ ,  $\kappa$ ) from CCN activity were 20 ~ 70 % higher than the that from sub-saturated 70 hygroscopicity, using oxidation of representative biogenic precursors, such as monoterpenes (Wex et al.,



2009;Liu et al., 2018;Zhao et al., 2016;Prenni et al., 2007), sesquiterpenes (Huff Hartz et al., 2005) and limonene (Zhao et al., 2016;Liu et al., 2018). They speculated that the higher measured CCN activity of the biogenic SOA may be caused by the complex composition and variable properties, such as the suppressed surface tension below that of the pure water induced by organic surfactants (Wex et al., 2009),  
75 the presence of sparingly soluble organic compounds (Petters et al., 2009;Prenni et al., 2007), non-ideality-driven liquid-liquid phase separation (Liu et al., 2018) or joint influences of these factors. In contrast, Duplissy et al. (2008) found a good reconciliation of hygroscopicity parameter  $\kappa$  between the hygroscopicity at 95 % RH and CCN activity of the SOA from  $\alpha$ -pinene oxidation. Moreover, Good et al. (2010b) found that the agreement of  $\kappa$  reconciliation of the SOA from  $\alpha$ -pinene ozonolysis was  
80 influenced by the use of three different custom-built Hygroscopicity Tandem Differential Mobility Analyser (HTDMA) for sub-saturated hygroscopicity measurements and the absence/presence of inorganic seed. For the anthropogenic or biogenic-anthropogenic mixed SOA, Zhao et al. (2016) observed a smaller discrepancy of  $\kappa$  than for the biogenic SOA, but the measured CCN activity was still higher than the sub-saturated hygroscopicity ( $> 20\%$ ). In contrast, Liu et al. (2018) found no discrepancy for  
85 anthropogenic SOA.

Clearly the complexity of aerosol chemical composition can propagate to their water uptake behaviour. Nevertheless, our understanding of the chemical controls on the sub- and super-saturated water uptake is not sufficient, especially for the evolution of the multi-component organic-inorganic systems. The rate of change of organic mass fraction in different systems may play an important role in aerosol water uptake.  
90 To improve our understanding on chemical controls of water uptake, we designed and performed a series of chamber experiments to investigate the evolution of the chemical composition, the sub- and super-saturated water uptake of SOA from single and mixed VOCs in the presence of ammonium sulphate seed. The goal of this paper was to explore the change and controlling factors in the water uptake of multicomponent seeded particles as they transformed through the oxidation of the various mixed VOC  
95 systems.



## 2 Materials and method

### 2.1 Experiment design

A series of chamber experiments were designed and conducted at Manchester Aerosol Chamber (MAC) to investigate the impacts of mixing VOCs on the SOA formation mechanisms and aerosol physicochemical properties (e.g. chemical composition, volatility, water uptake). An overview of the overall project could be found in Voliotis et al., (2021, ACP submitted, this issue). Briefly, this work builds on the concept explored in McFiggans et al. (2019) using a mixture of the biogenic SOA precursors,  $\alpha$ -pinene and isoprene, extended to a ternary system by including *o*-cresol as an anthropogenic VOC. *o*-cresol is both directly emitted anthropogenically or naturally and is a first generation oxidation product of toluene, both being abundant aromatic VOCs observed in anthropogenic polluted areas (Seinfeld and Pandis, 2016). *o*-cresol is sufficiently close in reactivity towards OH radical with  $\alpha$ -pinene and isoprene as to contribute comparable amounts of oxidation products to the mixture (Coeur-Tourneur et al., 2006;IUPAC). Additionally, it is a moderate SOA yield compound (Henry et al., 2008), so any interactions in the mixture with the oxidation products of the other VOCs may lead to contrasting interactions to those in the binary high-yield  $\alpha$ -pinene mixture with low-yield isoprene (McFiggans et al., 2019). VOCs were injected into the chamber with modest VOC/NO<sub>x</sub> ratio ranging 4 ~ 10 and the mixing ratio of VOCs were chosen such that they would have the same reactivity towards ·OH at the beginning of the experiment but not necessary afterwards when photochemistry starts. Ammonium sulphate particles were injected considering its abundance in atmosphere (Seinfeld and Pandis, 2016), as seeds for SOA condensation. Details of the initial conditions are shown in Table 1. It is worth noting that the single VOC isoprene experiments were carried out, but not included in this study since they had too low SOA yield to measure with no noticeable change to hygroscopicity.

A detailed description on characterisation of MAC facility (e.g. controlling condition stability, gas/particle wall loss, auxiliary mechanism, aerosol formation capability) can be found in Shao et al. (2021). Briefly, MAC consists of an 18 m<sup>3</sup> FEP Teflon bag supported by movable aluminium frames and runs as a batch reactor. The chamber is mounted inside the enclosure where the air conditioning system can well control the temperature ( $25 \pm 2$  °C) and relative humidity (RH,  $50 \pm 5$  %) in chamber in this



study. For photochemistry experiments, two 6kW Xenon arc lamps (XBO 6000 W/HSLA OFR, Osram) and 5 rows (#16 for each row) of halogen bulbs (Solux 50W/4700K, Solux MR16, USA) are used to  
125 mimic the solar spectrum of mid-day of clear sky conditions in June in Manchester and the total actinic  
flux between 290 and 600 nm was  $\sim 1/3$  of the clear-sky solar radiation  
(<https://www.eurochamp.org/simulation-chambers/MAC-MICC>). The chamber is kept clean through a  
reproducible cleaning protocol, including daily cleaning (overnight O<sub>3</sub> oxidation removal and automatic  
fill/flush physical cleaning cycles before and after experiments) and regular harsh cleaning with high  
130 concentration of O<sub>3</sub> under strong ultraviolet. During an experiment, seed particles and gas precursors are  
injected and well mixed through the high flow rate blower and kept well-mixed by the continual external  
agitation of conditioned air through the gap between the enclosure and chamber. VOCs ( $\alpha$ -pinene,  
isoprene, *o*-cresol; Sigma Aldrich, GC grade  $\geq 99.99$  % purity) are injected through a heated glass bulb  
to be vaporized and flushed into chamber with high purity nitrogen (ECD grade, 99.997 %). NO<sub>x</sub> (as  
135 mostly NO<sub>2</sub> in this study) injection is controlled by mass flow controller and water vapour is added  
properly mixing with a dry purified clean air to chamber to adjust the desired RH condition. A series of  
instruments were deployed to record gas precursors (VOC, NO<sub>x</sub>, O<sub>3</sub>) and physicochemical properties of  
seeded SOA. Details of key instruments used in this study can be found in Sec. 2.2.

140 Table 1. Experimental initial conditions of the various single and mixed biogenic and anthropogenic VOC systems  
photochemistry in the presence of ammonium sulphate seed.

Date	VOC type	[VOC] <sub>0</sub> (ppbV)	VOC/NO <sub>x</sub>	Seed conc. (ug/m <sup>3</sup> ) <sup>a</sup>
2019.03.29	$\alpha$ -pinene	309	7.2	67.6
2019.04.17	$\alpha$ -pinene	155	4.4	46.2
2019.07.13	$\alpha$ -pinene	103	5.7	55.4
2019.04.12	<i>o</i> -cresol	400	n.a.	40.9
2019.04.19	<i>o</i> -cresol	200	5.0	56.0
2019.07.10	<i>o</i> -cresol	133	4.9	38.1
2019.04.08	$\alpha$ -pinene/isoprene	237 (155/82)	9.9	50.5
2019.04.23	$\alpha$ -pinene/ <i>o</i> -cresol	355 (155/200)	5.9	42.5
2019.04.24	<i>o</i> -cresol/isoprene	282(82/200)	n.a.	57.0



---

2019.07.30	$\alpha$ -pinene/isoprene/o-cresol	191 (103/55/133)	3.7	45.9
------------	------------------------------------	------------------	-----	------

---

<sup>a</sup> calculated mass concentration from volume concentration from DMPS with a density of 1.77 g cm<sup>-3</sup>.

n.a. means no available data due to instrument failure.

## 2.2 Measurements

145 The measured aerosol particles are dried with a Nafion® drier (Perma Pure, MD-110-12, Toms River, NJ, USA) to RH < 30 % before introduced to the following instruments. The sub-saturated water uptake of aerosol particles was measured by a custom-built Hygroscopicity Tandem Differential Mobility Analyser (HTDMA) (Good et al., 2010a). The HTDMA is used to determine aerosol growth factor (GF) at a certain RH. Principally, sampled aerosol particles are dried and then selected by the first Differential  
150 Mobility Diameter (DMA1) to get monodisperse aerosol particles at given size ( $D_0$ ), which further are humidified at 90 % RH in this study. The humidified aerosol particles enter the second DMA and a Condensation Particle Counter (CPC) in order to determine the size distributions. The HTDMA was calibrated and its performance was validated by (NH<sub>4</sub>)<sub>2</sub>SO<sub>4</sub> before and after the campaign following the method of Good et al. (2010a). Finally, the growth factor probability density function and mean growth  
155 factor (GF) were retrieved using TDMA<sub>inv</sub> method developed by Gysel et al. (2009). To track particle growth, the measured particle size increased from 75 nm up to 300 nm, depending on the geometric mean diameter of aerosol populations during SOA formation evolution processes in various VOC systems.

The super-saturated water uptake of aerosol particles, that is the ability to activate to CCN, was measured by a DMT continuous flow CCN counter (Roberts and Nenes, 2005). In this study, the CCN counter was  
160 coupled with a DMA and a CPC to obtain the fraction of size-resolved aerosol particles activating to CCN ( $F_A$ ) at a certain supersaturation. Briefly, the DMA was used to select monodisperse dried aerosol particles (RH < 30 %), which are fed into the CCN counter and CPC in parallel to count the activated and total number concentrations of aerosol particles, respectively. During the experiments, DMA scans from 20 to 550 nm at supersaturation of 0.1 % ~ 0.5 % (varied with SOA formation process) were conducted.  $F_A$  as  
165 a function of the dry particle size ( $D_0$ ) was derived from the ratio of the activated and total aerosol particles



concentrations with a correction of DMA multiple charge. Finally, the particle size at 50 % activation ( $D_{CCCN}$ ) was identified through a sigmoid fit of  $F_A$ - $D_0$  curve, which was assumed to be the critical diameter at the critical supersaturation ( $S_{CCCN}$ ). CCN counter was calibrated and its performance was validated by  $(NH_4)_2SO_4$  before and after the campaign following the procedure in Good et al. (2010a).

170 The chemical composition of the non-refractory  $PM_{10}$  components (NR- $PM_{10}$ , including ammonium  $NH_4$ , sulphate  $SO_4$ , nitrate  $NO_3$ , SOA) was measured by a High-Resolution Time-of-Flight Aerosol Mass Spectrometer (HR-ToF-AMS, Aerodyne Research Inc., USA). Detailed instrument descriptions can be found elsewhere (DeCarlo et al., 2006; Jayne et al., 2000; Allan et al., 2004; Allan et al., 2003). During the experiment period, HR-ToF-AMS was calibrated and its performance was validated following the  
175 standard procedures (Jayne et al., 2000; Jimenez et al., 2003). In addition, to obtain the size-resolved chemical composition, a polystyrene latex sphere (PSL) calibration was performed to obtain the relationship between vacuum aerodynamic particle size and its velocity following the protocol provided at [http://cires1.colorado.edu/jimenez-group/wiki/index.php/Field\\_Data\\_Analysis\\_Guide](http://cires1.colorado.edu/jimenez-group/wiki/index.php/Field_Data_Analysis_Guide).

### 180 **2.3 $\kappa$ -Köhler approach**

The  $\kappa$ -Köhler approach is used to predict the CCN activity from the sub-saturated water uptake (Petters and Kreidenweis, 2007). Compared to the primitive Köhler theory (Köhler, 1936), the simplified  $\kappa$ -Köhler approach uses a single hygroscopicity parameter  $\kappa$  to describe the water activity in the Raoult term with assumptions of a constant dissociation factor of solutes and additivity of solutes without interactions  
185 (Petters and Kreidenweis, 2007). Therefore,  $\kappa$ -Köhler provides a single parameter  $\kappa$ , which can bridge the sub- and super-saturated water uptake, which is readily applied to predict cloud properties from aerosol physicochemical properties in climate models (Fanourgakis et al., 2019). However, it should be noted that the non-ideality of solution (e.g. the sparingly soluble SOA, molecular and ionic interactions), the potential influence of SOA on surface tension and the difference in co-condensation of condensable  
190 vapours through the systems will influence the results as previously discussed (Wex et al., 2009; Prenni et al., 2007; Hu et al., 2018), and which will be further discussed in the Sec. 3.4.





The hygroscopicity parameter  $\kappa$  from sub-saturated HTDMA and super-saturated CCN counter are referred as  $\kappa_{\text{HTDMA}}$  and  $\kappa_{\text{CCN}}$ , respectively.  $\kappa_{\text{HTDMA}}$  was calculated directly through Eq. [1-2] with the measured GF and dry particle size  $D_0$ . For CCN measurement,  $\kappa_{\text{CCN}}$  was derived from the computed  $\kappa$ -  
195 Dc-Sc relationship at surface tension of water and temperature of 298.15 K in Petters and Kreidenweis (2007). Here, Dc and Sc represent the dry diameter of aerosol particle and the critical supersaturation ratio of water vapour (maxima of the Köhler curve) to activate it to CCN.

$$S(D) = \frac{D^3 - D_0^3}{D^3 - D_0^3(1 - \kappa)} \exp\left(\frac{4\sigma M_w}{RT\rho_w D}\right) \quad [1]$$

$$D = D_0 GF \quad [2]$$

200 Where  $S(D)$  is the supersaturation ratio or RH at sub-saturated condition.  $D$  and  $D_0$  represents the dry and wet particle diameter, respectively.  $\sigma$ ,  $M_w$ ,  $\rho_w$  are droplet surface tension, molecular weight, and density of water, respectively.  $R$  and  $T$  represents the universal gas constant and absolute temperature, respectively. GF is the growth factor at 90 % RH measured by HTDMA.

## 205 **3 Results and Discussion**

### **3.1 Bulk and size-dependent chemical composition**

Fig. 1 and Fig. 2 show the bulk NR-PM<sub>1</sub> species and size-resolved organic mass fraction ( $\text{MR}_{\text{SOA/PM}}$ ) measured by HR-ToF-AMS, respectively. At the beginning of experiments before illumination (-1 ~ 0 h), seed particles are mainly comprised of sulphate with a small contribution from nitrate (Max. 5 % ~ 16 %  
210 of NR-PM<sub>1</sub>) in all investigated VOC systems. The observed nitrate was mainly inorganic ammonium nitrate and the organic nitrate was statistically insignificant (a detailed estimation method and discussion can be found in Wang et al. (2021)). Considering the small fraction of nitrate in the inorganic seed particles in this study and comparable water uptake ability with sulphate (Kreidenweis and Asa-Awuku, 2014), it may be expected that the overall hygroscopicity and CCN activity will be highly related to the  
215  $\text{MR}_{\text{SOA/PM}}$ . After initiating illumination, the condensable organic vapours were formed from VOCs photo-



oxidation, which further condensed on the inorganic seed particles yielding SOA. Therefore, an increasing  $MR_{SOA/PM}$  over time was observed, as shown in Fig. 1. As different VOC systems have different SOA yield and reactivity with oxidants, and the oxidation conditions varied in the different systems (see Voliotis et al., ACP submitted, this issue), the mass and the production rate of SOA varied with the VOC systems. After a six-hour photochemistry for the single VOC systems, the  $MR_{SOA/PM}$  approached  $0.88 \pm 0.01$ ,  $0.82 \pm 0.01$ ,  $0.62 \pm 0.01$ ,  $0.71 \pm 0.01$ ,  $0.56 \pm 0.02$  and  $0.52 \pm 0.02$  (last 0.5 h of experiments, avg.  $\pm$  std.) in the  $\alpha$ -pinene, 50 % reactivity  $\alpha$ -pinene, 33 % reactivity  $\alpha$ -pinene, *o*-cresol, 50 % reactivity *o*-cresol and 33 % reactivity *o*-cresol systems, respectively. For the binary and ternary systems, the  $MR_{SOA/PM}$  was  $0.79 \pm 0.01$ ,  $0.82 \pm 0.01$ ,  $0.32 \pm 0.01$  and  $0.78 \pm 0.01$  in the  $\alpha$ -pinene/isoprene,  $\alpha$ -pinene/*o*-cresol, *o*-cresol/isoprene, and  $\alpha$ -pinene/*o*-cresol/isoprene, respectively. Moreover, a size-dependent chemical composition was observed, with a higher  $MR_{SOA/PM}$  in smaller particle size in all investigated VOC systems (as shown in Fig. 2). This indicates that the chemical composition is not uniform across the size distribution. As the inorganic compounds are much more hygroscopic than the SOA (Kreidenweis and Asa-Awuku, 2014; Prenni et al., 2007; Alfarra et al., 2013; Alfarra et al., 2012), aerosol hygroscopicity and CCN activity will vary with  $MR_{SOA/PM}$ . Considering measured dry size differences between the HTDMA and CCN counter, size-resolved chemical composition has been used to ensure that the paired  $\kappa_{HTDMA}$  and  $\kappa_{CCN}$  for measurement reconciliation are with comparable  $MR_{SOA/PM}$ .

### 3.2 Aerosol hygroscopicity under sub-saturated conditions

The GF at 90 % RH was measured by a HTDMA and hygroscopicity parameter ( $\kappa_{HTDMA}$ ) was calculated using the  $\kappa$ -Köhler approach (Petters and Kreidenweis, 2007) for all the investigated VOC systems as shown in Fig. 3. Before the photochemistry with inorganic seed only, the GF at 90 % RH ( $\kappa_{HTDMA}$ ) for the 75 / 100 nm aerosol particles were 1.65 ~ 1.72 (0.45 ~ 0.50) in all VOC systems. This result is comparable with the predicted GF ( $\kappa_{HTDMA}$ ) of 1.71 ~ 1.72 (0.50 ~ 0.51) using UManSysProp (<http://umansysprop.seaes.manchester.ac.uk/>; Hygroscopic growth factor [inorganic system] scheme) (Topping et al., 2016). Here, the input to UManSysProp was the  $(NH_4)_2SO_4 + NH_4NO_3$  (0 ~ 10 %) observed in Sec. 3.1 with an assumption of non-ideality. After the commencement of photochemistry, the



MR<sub>SOA/PM</sub> increased over time. Consequently, the GF ( $\kappa_{\text{HTDMA}}$ ) decreased accordingly due to the less  
hygroscopic nature of SOA than inorganic compounds (Kreidenweis and Asa-Awuku, 2014; Prenni et al.,  
245 2007; Alfarra et al., 2013; Alfarra et al., 2012; Varutbangkul et al., 2006).

As expected, the rate of change and magnitude of the GF ( $\kappa_{\text{HTDMA}}$ ) decreases over time depends on the  
change of MR<sub>SOA/PM</sub> in all VOC systems. For example, for the  $\alpha$ -pinene system, the MR<sub>SOA/PM</sub> increased  
substantially from  $\sim 0$  to 0.72 within an hour of the experiment (as shown in Fig. 1 a1), correspondingly,  
the GF ( $\kappa_{\text{HTDMA}}$ ) decreased from 1.65  $\sim$  1.72 (0.45  $\sim$  0.50) to  $\sim$  1.15 ( $\sim$  0.1) (as shown in Fig. 3 a1). In  
250 comparison, for *o*-cresol/isoprene system, it took six hours for the MR<sub>SOA/PM</sub> to increase to 0.33, and  
accordingly, the GF ( $\kappa_{\text{HTDMA}}$ ) decreased slowly to 1.44  $\sim$  1.53 (0.28  $\sim$  0.36) after the six-hour experiment.  
Moreover, consistent with the observed higher MR<sub>SOA/PM</sub> for smaller size in Sec. 3.1, Fig. 3 shows  
evidence that the GF ( $\kappa_{\text{HTDMA}}$ ) is size-dependent, with up to  $\sim 0.2$  ( $\sim 0.1$ ) lower in 100 nm aerosol particles  
than the 200 nm measured adjacently. This is consistent with the non-uniform size-dependent particle  
255 chemical composition in our chamber studies. Consideration of size-resolved chemical composition is  
very important for the aerosol physical and optical properties where both chemical composition and  
particle size can play a role.

### 3.3 CCN potential under super-saturated conditions

260 CCN activity above water saturation was simultaneously recorded by CCN counter during the  
experiments of all investigated VOC systems. Fig. 4 shows the relationship of the critical supersaturation  
of water vapour ( $S_c$ ), the dry particle size and the  $\kappa_{\text{CCN}}$ . It provides the required  $S_c$  to activate 50 % of a  
given size of dry particles ( $D_{\text{CCN}}$ ), for which this CCN activation potential can be represented by a single  
hygroscopicity parameter ( $\kappa_{\text{CCN}}$ ) (Petters and Kreidenweis, 2007). At the beginning of experiments before  
265 photochemistry, the  $\kappa_{\text{CCN}}$  was mainly 0.55  $\sim$  0.65 in all investigated VOC systems, which is comparable  
with predicted  $\kappa$  of 0.58  $\sim$  0.64 for 50  $\sim$  100 nm from UManSysProp (CCN activation potential [inorganic  
system] scheme). After initiating photochemistry, a declining trend of  $\kappa_{\text{CCN}}$  over time was observed as  
the continuous condensation of less hygroscopic / CCN-active SOA, consistent with the trends of sub-



saturated water uptake in Sec. 3.2. For example, for the  $\alpha$ -pinene system as shown in Fig. 4 a1, the  $\kappa_{CCN}$  decreased from 0.64 to  $\sim 0.1$  within an hour whereas the  $\kappa_{CCN}$  decreased from 0.55 to 0.23 after the six-hour oxidation for the *o*-cresol/isoprene system. This significant differences between different VOC systems are highly related to the production rate of SOA and the corresponding change of  $MR_{SOA/PM}$  over time. It is worth noting that the set-point  $Sc$  in CCN counter was changed from 0.1  $\sim$  0.5 % during the experiments to follow the particle growth and ensure sufficient data points are collected for the activation curve to accurately determine the  $D_{CCN}$ .

### 3.4 CCN prediction from the sub-saturated conditions

This section illustrates the reconciliation of the aerosol hygroscopicity and CCN activity, and its relationship with the aerosol chemical composition in various VOC systems to investigate the performance of the  $\kappa$ -Köhler approach in predicting CCN activity from sub-saturated aerosol hygroscopicity. As shown in Sec. 3.1-3.2, the aerosol chemical composition is size-dependent. It is essential to ensure the chemical composition are comparable for HTDMA and CCN measurements for the reconciliation study if their measured dry particle sizes are different. Therefore, we selected the synchronized HTDMA/CCN data pairs only when the 10-min moving average of  $MR_{SOA/PM}$  for the measured particle sizes were within 5 %. An example of selected data pairs in the  $\alpha$ -pinene/isoprene/*o*-cresol system was shown in Fig. S1. In addition to the hygroscopicity parameter  $\kappa$ , the critical diameter ( $D_{CHpre}$ ) was predicted from  $\kappa_{HTDMA}$  under the critical supersaturation of the paired CCN measurement. Further, by assuming all particles larger than  $D_{CHpre}$  will be activated at the given critical supersaturation, the CCN number was predicted based on the predicted  $D_{CHpre}$  and particle number size distribution.

Fig. 5 shows a summary of (a)  $\kappa_{HTDMA}$ , (b)  $\kappa_{CCN}$ , (c)  $\kappa_{HTDMA}/\kappa_{CCN}$ , (d)  $\kappa_{HTDMA}-\kappa_{CCN}$ , (e)  $D_{CHpre}/D_{CCN}$ , and (f)  $N_{ccn_{Hpre}}/N_{ccn_{CCN}}$  as a function of the organic mass fraction in various VOC systems (except for  $\alpha$ -pinene and 33 %  $\alpha$ -pinene systems due to CCN instrument failure). Similar trends of the investigated parameters as a function of  $MR_{SOA/PM}$  were observed in all VOC systems. As shown in panel a-b, the hygroscopicity parameter  $\kappa_{HTDMA}$  and  $\kappa_{CCN}$  decreased with the increase of  $MR_{SOA/PM}$  in all VOC systems, indicating aerosol particles became less hygroscopic and CCN-active modified by the increasingly



condensed SOA. For a summary of all data points binned with a  $MR_{SOA/PM}$  of 0.1, the black solid circles and grey lines represent the average and standard deviation of the categorized data points. The overall  $\kappa_{HTDMA}$  ( $\kappa_{CCN}$ ) declined from  $0.46 \pm 0.02$  ( $0.61 \pm 0.07$ ) to  $0.14 \pm 0.03$  ( $0.09 \pm 0.01$ ) when the  $MR_{SOA/PM}$  increased from  $\sim 0$  to  $\sim 0.8$ .

300 In addition to the overall trend, the differences of  $\kappa_{HTDMA}$  ( $\kappa_{CCN}$ ) at the same  $MR_{SOA/PM}$  in the various VOC systems indicated that the SOA composition played a second-order role in the hygroscopicity (CCN activity). A higher  $\kappa_{HTDMA}$  ( $\kappa_{CCN}$ ) of the multi-component SOA-inorganic mixtures at the same level of  $MR_{SOA/PM}$  indicated a higher  $\kappa$  of the SOA, according to the ZSR mixing rule of  $\kappa$  demonstrated in Petters and Kreidenweis (2007). In this study, the  $\kappa_{HTDMA}$  ( $\kappa_{CCN}$ ) (indicating a higher  $\kappa$  of the SOA), in the  $\alpha$ -  
305 pinene/isoprene/*o*-cresol and 33 % *o*-cresol systems were the highest, which are higher than other VOC systems by  $0 \sim 0.2$  ( $0 \sim 0.3$ ), depending on the  $MR_{SOA/PM}$ . In contrast, the  $\kappa_{HTDMA}$  ( $\kappa_{CCN}$ ) in *o*-cresol and 50 % reactivity *o*-cresol were usually the lowest at the same level of  $MR_{SOA/PM}$ , whereas the 50 % reactivity  $\alpha$ -pinene,  $\alpha$ -pinene/isoprene and *o*-cresol/isoprene seated in the middle. Previous studies found the sub-saturated aerosol water uptake ( $\kappa$ ) increases with chemical aging of SOA from single precursor  
310 oxidation and showed a positive relationship with SOA oxidation state (e.g. O:C ratio or f44, fraction of m/z 44 in total organic signal) (Jimenez et al., 2009;Massoli et al., 2010;Lambe et al., 2011;Zhao et al., 2016;Duplissy et al., 2011), but no clear relationship involving multiple precursors with various oxidation state (Alfarra et al., 2013;Zhao et al., 2016). In this study, it can be seen from the Fig. S2 that the trends of the declining f44 with the  $MR_{SOA/PM}$  were similar in  $\alpha$ -pinene/isoprene/*o*-cresol, 33 % *o*-cresol, 50 %  
315 reactivity  $\alpha$ -pinene and  $\alpha$ -pinene/isoprene systems but showed different patterns in the *o*-cresol/isoprene, *o*-cresol and 50 % reactivity *o*-cresol systems (the f44 were higher than the other four systems at the same  $MR_{SOA/PM}$ ). The oxidation state of SOA (f44) showed no clear relationship with the observed  $\kappa$  trends in various VOC systems as shown in Fig. 5 a-b, which is consistent with previous studies involving multiple precursors (Alfarra et al., 2013;Zhao et al., 2016). Other factors might have influences but need further  
320 investigations, such as organic mass loading, molecular weight (Cappa et al., 2011;Petters et al., 2017), solubility (Petters et al., 2009;Ruehl and Wilson, 2014;Huff Hartz et al., 2006), surface tension (Ovadnevaite et al., 2017;Bzdek et al., 2020;Ruehl et al., 2016;Lowe et al., 2019) and co-condensation (Kulmala et al., 1993;Topping et al., 2013b;Hu et al., 2018).



Panel c-d in Fig. 5 shows the ratio ( $\kappa_{\text{HTDMA}}/\kappa_{\text{CCN}}$ ) and the absolute difference ( $\kappa_{\text{HTDMA}}-\kappa_{\text{CCN}}$ ) of  $\kappa$  derived  
325 from HTDMA and CCN counter as a function of  $\text{MR}_{\text{SOA/PM}}$ . Interestingly, a clear co-increase of  
 $\kappa_{\text{HTDMA}}/\kappa_{\text{CCN}}$  ( $\kappa_{\text{HTDMA}}-\kappa_{\text{CCN}}$ ) with the  $\text{MR}_{\text{SOA/PM}}$  was observed in all VOC systems. The overall  
 $\kappa_{\text{HTDMA}}/\kappa_{\text{CCN}}$  for all VOC systems increased from  $0.76 \pm 0.08$  to  $1.62 \pm 0.26$  with the  $\text{MR}_{\text{SOA/PM}}$  increasing  
from  $\sim 0$  to  $\sim 0.8$ , and correspondingly, the  $\kappa_{\text{HTDMA}}-\kappa_{\text{CCN}}$  increased from  $-0.15 \pm 0.06$  to  $0.05 \pm 0.02$ . This  
330 means the averaged  $\kappa_{\text{HTDMA}}$  was  $\sim 25\%$  ( $16\% \sim 32\%$ ) lower than  $\kappa_{\text{CCN}}$  with inorganic compounds at the  
beginning of the experiments, but this discrepancy decreased down to  $\sim 0$  with the increasing  $\text{MR}_{\text{SOA/PM}}$   
and even became higher than  $\kappa_{\text{CCN}}$  by  $\sim 60\%$  ( $36\% \sim 88\%$ ) at  $\text{MR}_{\text{SOA/PM}}$  of  $\sim 0.8$ . These results indicated  
that the performances of  $\kappa$ -Köhler approach on the reconciliation study of sub- and super-saturated water  
uptake varied with the  $\text{MR}_{\text{SOA/PM}}$ .

The discrepancy in the  $\kappa_{\text{HTDMA}}$  and  $\kappa_{\text{CCN}}$  can influence the prediction of CCN activity from sub-saturated  
335 hygroscopicity ( $\kappa_{\text{HTDMA}}$ ) using the  $\kappa$ -Köhler approach. As shown in Fig. 5 e-f, the predicted critical  
diameter ( $D_{\text{CHpre}}$ ) was  $5 \sim 20\%$  (avg.  $\sim 10\%$ ) higher than the measured  $D_{\text{CCN}}$  at  $\text{MR}_{\text{SOA/PM}}$  of 0.02, and  
the  $D_{\text{CHpre}}/D_{\text{CCN}}$  decreased gradually to  $0.8 \sim 1$  (avg.  $\sim 0.9$ ) as  $\text{MR}_{\text{SOA/PM}}$  approached 0.8. As a result, the  
predicted CCN number concentration from sub-saturated water uptake was underestimated by  $0 \sim 20\%$   
(avg.  $\sim 10\%$ ) at  $\text{MR}_{\text{SOA/PM}}$  of 0.02. This underestimation of CCN number became weaker (averaged value  
340 almost down to  $\sim 0$ ) with  $\text{MR}_{\text{SOA/PM}}$  increased to  $0.2 \sim 0.4$  due to SOA condensation, and it even turned  
the underestimation to an overestimation by up to  $40\%$  (avg.  $20\%$ ) with  $\text{MR}_{\text{SOA/PM}}$  of  $\sim 0.8$ . It is worth  
noting that the prediction of critical diameter and CCN number concentration from  $\kappa_{\text{HTDMA}}$  are based on  
the concurrently measured critical supersaturation and particle number size distribution. The broader  
influences of the observed trend of  $\kappa_{\text{HTDMA}}/\kappa_{\text{CCN}}$  as a function of  $\text{MR}_{\text{SOA/PM}}$  on CCN activity prediction  
345 can vary a lot under different conditions of supersaturation and particle size distribution, which need  
further investigations.



### 3.5 Discussion on the $\kappa$ discrepancy during measurement reconciliation

As demonstrated above, the  $\kappa_{\text{HTDMA}}$  was, on average,  $\sim 25\%$  lower than the  $\kappa_{\text{CCN}}$  of the inorganic seeds  
350 when the  $\text{MR}_{\text{SOA/PM}}$  was  $\sim 0$ , which was consistent with the thermodynamic model results from  
UManSysProp (Topping et al., 2016) with an assumption of non-ideality (both  $\kappa$  were 0.72 if assuming  
ideality). This indicates that the non-ideality could play an important role in the differences of  $\kappa$  derived  
from the two instruments and that the instruments are sufficiently sensitive to resolve non-ideal effects in  
the inorganic systems. Interestingly, this  $\kappa$  discrepancy changed in the evolution of SOA formation in all  
355 investigated VOC systems, with the average  $\kappa_{\text{HTDMA}}/\kappa_{\text{CCN}}$  increasing from 0.76 to 1.62 when the  
 $\text{MR}_{\text{SOA/PM}}$  increased from  $\sim 0$  to  $\sim 0.8$ .

Multiple factors could influence the  $\kappa$  reconciliation between the sub- and super-saturated water uptake  
in different ways due to the complexity of condensed SOA and the simplified assumptions used in the  $\kappa$ -  
Köhler approach (e.g. surface tension of water, fully dissolution, ideality, water vapour as the only  
360 condensable compound). Previous studies found that some organic compounds are surface-active which  
can suppress the surface tension up to a third of the water (Shulman et al., 1996; Facchini et al., 1999).  
Due to the wide solubility of the organic compounds (Hallquist et al., 2009), organic compounds with  
limited solubility can dissolve more with the increase of the aerosol liquid water and the surrounding  
water saturation. This surface tension suppression or the sparingly soluble organic compounds could  
365 facilitate the CCN activation (Wex et al., 2009; Petters et al., 2009; Prenni et al., 2007; Facchini et al.,  
1999; Shulman et al., 1996). In addition, Liu et al. (2018) measured the sub- and super-saturated water  
uptake of nucleated SOA and compared with thermodynamic models, and found that the non-ideality-  
driven liquid-liquid phase separation in biogenic-SOA could be the reason for the higher  $\kappa$  from CCN  
whereas no phase separation in anthropogenic-SOA might explain a good agreement of the reconciliation.  
370 But all above evidence points to the same direction of a higher or equivalent CCN activity ( $\kappa_{\text{CCN}}$ ) than the  
sub-saturated condition ( $\kappa_{\text{HTDMA}}$ ), which cannot explain the observed trend in this study (the faster  
decrease of  $\kappa_{\text{CCN}}$  relative to the  $\kappa_{\text{HTDMA}}$  with increasing  $\text{MR}_{\text{SOA/PM}}$ ).

The non-ideality of the solutes at different water saturation conditions and the different co-condensation  
of semi-volatile compounds within the two instruments could be the possible reasons for the increasing



375 trend of  $\kappa_{\text{HTDMA}}/\kappa_{\text{CCN}}$  with  $\text{MR}_{\text{SOA/PM}}$ . The non-ideal activity coefficient of compounds varied from the concentrated solutions at 90% RH within the HTDMA to the diluted ones at super-saturated conditions within CCN counter (Brechtel and Kreidenweis, 2000a, b). Additionally, the interactions of inorganic ions and organic molecules can exert both positive and negative effects in the water uptake, depending on the organic fraction and inorganic species (Cruz and Pandis, 2000). With assuming the ideality in the  
380  $\kappa$  derived from the sub- and super-saturated conditions, the varied organic fraction in the evolution of SOA formation in various VOC systems could yield a changing non-ideal activity coefficient and further may influence the  $\kappa$  reconciliation of the two instruments. Moreover, the semi-volatile compounds (e.g. organics,  $\text{HNO}_3$ ) can co-condense with water vapour on aerosol particles and enhance the water uptake (Rudolf et al., 1991; Hu et al., 2018; Topping et al., 2013b; Wang et al., 2019; Gunthe et al., 2021). But the  
385 differences in the design of the HTDMA and CCN counter result in different levels of response to the co-condensation effect. The sampled aerosols from chamber were dried to  $\text{RH} < 30\%$  before splitting and entering into the HTDMA and CCN counter. During the drying process, semi-volatile compounds can co-evaporate with water vapour to the gaseous phase and water vapour was then removed through the Nafion membrane, but this will have the same influences on both instruments anyway. In our setup, the  
390 sheath air of first DMA in both instruments were close-loop, which means that the sheath air will reach equilibrium with the sample air including gaseous organic compounds. After selecting a given size of aerosols by the first DMA, the aerosols went through the conditioned humid environment. The temperature was decreased to  $18\text{ }^\circ\text{C}$  to reach the set RH in HTDMA (Good et al., 2010a), which will facilitate the co-condensation of the semi-volatile compounds and the growth of the aerosol particles by  
395 lowering the saturation vapour pressure due to temperature drop (Hu et al., 2018). However, the temperature in CCN counter was designed to increase to keep a certain water saturation (Roberts and Nenes, 2005; Good et al., 2010a), which is not favourable for the co-condensation effect. Further investigations are needed to clearly understand the impacts of these two factors on the reconciliation of the sub- and super-saturated water uptake using  $\kappa$ -Köhler approach or further improvement on method.





## 400 **4 Conclusions**

In this study, we designed and performed a series of chamber experiments to improve our understanding of the chemical controls of the sub- and super-saturated water uptake in the evolution of the SOA formation from mixed precursors in the presence of ammonium sulphate seed. The yield and reactivity of the SOA precursors controlled the SOA production rate in different VOC systems, and therefore the increase of organic mass fraction ( $MR_{SOA/PM}$ ). Our results showed that the  $MR_{SOA/PM}$  is the main factor  
405 influencing the hygroscopicity and CCN activity in terms of  $\kappa$ , and the SOA composition plays a second-order role. At the same level of  $MR_{SOA/PM}$ , the order of  $\kappa_{HTDMA}$  and  $\kappa_{CCN}$  were  $\alpha$ -pinene/isoprene/o-cresol and 33 % o-cresol >  $\alpha$ -pinene,  $\alpha$ -pinene/isoprene and o-cresol/isoprene > o-cresol and 50 % reactivity o-cresol systems.

410 During the SOA formation process in all VOC systems, size-resolved chemical composition was observed, for which the smaller particles have higher  $MR_{SOA/PM}$ . To avoid the influences of composition differences on the reconciliation study of sub- and super-saturated water uptake, the synchronized HTDMA and CCN data pairs with a comparable chemical composition were selected according to the size-resolved chemical composition.

415 In the reconciliation, we found the discrepancy between  $\kappa_{HTDMA}$  and  $\kappa_{CCN}$  varied with the  $MR_{SOA/PM}$ . Consequently, the performance of the  $\kappa$ -Köhler approach on CCN activity prediction from sub-saturated condition also changed with the  $MR_{SOA/PM}$ . This trend was observed in all investigated VOC systems, regardless of the VOC sources and initial concentrations. For all investigated VOC systems, the averaged  $\kappa_{HTDMA}/\kappa_{CCN}$  increased from  $0.76 \pm 0.08$  to  $1.62 \pm 0.26$  when the  $MR_{SOA/PM}$  increased from  $\sim 0$  to  $\sim 0.8$ ,  
420 meanwhile the mean absolute difference ( $\kappa_{HTDMA}-\kappa_{CCN}$ ) increased from  $-0.15 \pm 0.06$  to  $0.05 \pm 0.02$ . This varying  $\kappa_{HTDMA}/\kappa_{CCN}$  with  $MR_{SOA/PM}$  cannot be explained by the CCN activity favouring factors such as the suppression surface tension or the sparingly soluble properties of organic compounds. The non-ideality of organic-inorganic solutes or differences in the way that the instruments respond to co-condensation of condensable vapours could be possible reasons but need further investigations.

425 In addition, we estimated the influences of this  $\kappa$  discrepancy trend on the prediction of CCN activity from the sub-saturated hygroscopicity ( $\kappa_{HTDMA}$ ). The predicted mean CCN number concentration was



underestimated by  $\sim 10\%$  at  $MR_{SOA/PM}$  of  $\sim 0$ . This underestimation of CCN number disappeared with an increase of  $MR_{SOA/PM}$  to  $0.2 \sim 0.4$  due to SOA condensation, and ultimately turned to an overestimation by  $\sim 20\%$  in average with  $MR_{SOA/PM}$  of  $\sim 0.8$ . It is worth noting that the influences of the  $\kappa$  discrepancy trend on CCN activity prediction were estimated based on the current measurements of critical supersaturation and particle number size distribution. Broader impacts of this chemical-dependent performance of the  $\kappa$ -Köhler approach in cloud properties prediction under various atmospheric conditions should be considered in climate models to better project aerosol-induced climate effect.

#### 435 **Data availability**

The observational dataset of this study is open-access through EUROCHAMP-2020 programme (<https://data.eurochamp.org/data-access/chamber-experiments/>).

#### **Author contributions**

440 Y.W. conceived this study. G.M., M.R.A., Y.W., A.V. and Y.S. co-designed the chamber experiments. Y.W., A.V., Y.S. and D.M. conducted the chamber experiments. D.H. offered in-kind trainings on operation and data analysis of HTDMA and CCN counter for Y.W. During chamber experiments, Y.W. performed HTDMA and CCN counter measurements used in this study, conducted data integration and analysis, and wrote the manuscript. Y.C. provided helpful discussions. G.M. and M.R.A. proofread and  
445 improved the manuscript.



## Acknowledgement

Manchester Aerosol Chamber acknowledges the financial support from EUROCHAMP 2020. We acknowledge AMF/AMOF for providing SMPS instrument (AMF\_25072016114543 and AMF\_04012017142558). Y.W. acknowledges the joint scholarship of The University of Manchester and Chinese Scholarship Council. M.R.A. acknowledges support by UK National Centre for Atmospheric Sciences (NACS) funding. A.V. acknowledges the Natural Environment Research Council (NERC) EAO Doctoral Training Partnership funding.

## References

- 455 Alfarra, M. R., Hamilton, J. F., Wyche, K. P., Good, N., Ward, M. W., Carr, T., Barley, M. H., Monks, P. S., Jenkin, M. E., Lewis, A. C., and McFiggans, G. B.: The effect of photochemical ageing and initial precursor concentration on the composition and hygroscopic properties of  $\beta$ -caryophyllene secondary organic aerosol, *Atmos. Chem. Phys.*, 12, 6417-6436, 10.5194/acp-12-6417-2012, 2012.
- 460 Alfarra, M. R., Good, N., Wyche, K. P., Hamilton, J. F., Monks, P. S., Lewis, A. C., and McFiggans, G.: Water uptake is independent of the inferred composition of secondary aerosols derived from multiple biogenic VOCs, *Atmos. Chem. Phys.*, 13, 11769-11789, 10.5194/acp-13-11769-2013, 2013.
- Allan, J. D., Jimenez, J. L., Williams, P. I., Alfarra, M. R., Bower, K. N., Jayne, J. T., Coe, H., and Worsnop, D. R.: Quantitative sampling using an Aerodyne aerosol mass spectrometer 1. Techniques of data interpretation and error analysis, *Journal of Geophysical Research: Atmospheres*, 108, 10.1029/2002jd002358, 2003.
- 465 Allan, J. D., Delia, A. E., Coe, H., Bower, K. N., Alfarra, M. R., Jimenez, J. L., Middlebrook, A. M., Drewnick, F., Onasch, T. B., Canagaratna, M. R., Jayne, J. T., and Worsnop, D. R.: A generalised method for the extraction of chemically resolved mass spectra from Aerodyne aerosol mass spectrometer data, *Journal of Aerosol Science*, 35, 909-922, <https://doi.org/10.1016/j.jaerosci.2004.02.007>, 2004.
- 470 Bellouin, N., Quaas, J., Gryspeerdt, E., Kinne, S., Stier, P., Watson-Parris, D., Boucher, O., Carslaw, K. S., Christensen, M., Daniau, A.-L., Dufresne, J.-L., Feingold, G., Fiedler, S., Forster, P., Gettelman, A., Haywood, J. M., Lohmann, U., Malavelle, F., Mauritsen, T., McCoy, D. T., Myhre, G., Mülmenstädt, J., Neubauer, D., Possner, A., Rugenstein, M., Sato, Y., Schulz, M., Schwartz, S. E., Sourdeval, O., Storelvmo, T., Toll, V., Winker, D., and Stevens, B.: Bounding Global Aerosol Radiative Forcing of Climate Change, *Reviews of Geophysics*, 58, e2019RG000660, <https://doi.org/10.1029/2019RG000660>, 2020.



- 475 Boucher, O., Randall D., Artaxo P., Bretherton C., Feingold G., Forster P., Kerminen V.-M., Kondo Y., Liao H., Lohmann U., Rasch P., Satheesh S.K., Sherwood S., B., S., and X.Y., Z.: Clouds and Aerosols. In: *Climate Change 2013: The Physical Science Basis. Contribution of Working Group I to the Fifth Assessment Report of the Intergovernmental Panel on Climate Change* [Stocker, T.F., D. Qin, G.-K. Plattner, M. Tignor, S.K. Allen, J. Boschung, A. Nauels, Y. Xia, V. Bex and P.M. Midgley (eds.)], in, Cambridge University Press, Cambridge, United Kingdom and New York, NY, USA, 571–658, 2013.
- 480 Brechtel, F. J., and Kreidenweis, S. M.: Predicting Particle Critical Supersaturation from Hygroscopic Growth Measurements in the Humidified TDMA. Part I: Theory and Sensitivity Studies, *Journal of the Atmospheric Sciences*, 57, 1854-1871, 10.1175/1520-0469(2000)057<1854:Ppcsfh>2.0.Co;2, 2000a.
- Brechtel, F. J., and Kreidenweis, S. M.: Predicting Particle Critical Supersaturation from Hygroscopic Growth Measurements in the Humidified TDMA. Part II: Laboratory and Ambient Studies, *Journal of the Atmospheric Sciences*, 57, 1872-1887, 10.1175/1520-0469(2000)057<1872:Ppcsfh>2.0.Co;2, 2000b.
- 485 Bzdek, B. R., Reid, J. P., Malila, J., and Prisle, N. L.: The surface tension of surfactant-containing, finite volume droplets, *Proceedings of the National Academy of Sciences*, 117, 8335-8343, 10.1073/pnas.1915660117, 2020.
- Cappa, C. D., Che, D. L., Kessler, S. H., Kroll, J. H., and Wilson, K. R.: Variations in organic aerosol optical and hygroscopic properties upon heterogeneous OH oxidation, *Journal of Geophysical Research: Atmospheres*, 116, <https://doi.org/10.1029/2011JD015918>, 2011.
- 490 Coeur-Tourneur, C., Henry, F., Janquin, M.-A., and Brutier, L.: Gas-phase reaction of hydroxyl radicals with m-, o- and p-cresol, *International Journal of Chemical Kinetics*, 38, 553-562, 10.1002/kin.20186, 2006.
- Cruz, C. N., and Pandis, S. N.: The effect of organic coatings on the cloud condensation nuclei activation of inorganic atmospheric aerosol, *Journal of Geophysical Research: Atmospheres*, 103, 13111-13123, 10.1029/98JD00979, 1998.
- 495 Cruz, C. N., and Pandis, S. N.: Deliquescence and hygroscopic growth of mixed inorganic - Organic atmospheric aerosol, *Environmental Science and Technology*, 34, 4313-4319, 10.1021/es9907109, 2000.
- DeCarlo, P. F., Kimmel, J. R., Trimborn, A., Northway, M. J., Jayne, J. T., Aiken, A. C., Gonin, M., Fuhrer, K., Horvath, T., Docherty, K. S., Worsnop, D. R., and Jimenez, J. L.: Field-Deployable, High-Resolution, Time-of-Flight Aerosol Mass Spectrometer, *Analytical Chemistry*, 78, 8281-8289, 10.1021/ac061249n, 2006.
- 500 Duplissy, J., Gysel, M., Alfarra, M. R., Dommen, J., Metzger, A., Prevot, A. S. H., Weingartner, E., Laaksonen, A., Raatikainen, T., Good, N., Turner, S. F., McFiggans, G., and Baltensperger, U.: Cloud forming potential of secondary organic aerosol under near atmospheric conditions, *Geophysical Research Letters*, 35, 10.1029/2007GL031075, 2008.
- 505 Duplissy, J., DeCarlo, P. F., Dommen, J., Alfarra, M. R., Metzger, A., Barmapadimos, I., Prevot, A. S. H., Weingartner, E., Tritscher, T., Gysel, M., Aiken, A. C., Jimenez, J. L., Canagaratna, M. R., Worsnop, D. R., Collins, D. R., Tomlinson, J., and Baltensperger, U.: Relating hygroscopicity and composition of organic aerosol particulate matter, *Atmos. Chem. Phys.*, 11, 1155-1165, 10.5194/acp-11-1155-2011, 2011.



- Ervens, B., Cubison, M., Andrews, E., Feingold, G., Ogren, J. A., Jimenez, J. L., DeCarlo, P., and Nenes, A.: Prediction of cloud condensation nucleus number concentration using measurements of aerosol size distributions and composition and light scattering enhancement due to humidity, *Journal of Geophysical Research: Atmospheres*, 112, 10.1029/2006JD007426, 2007.
- 510 Facchini, M. C., Mircea, M., Fuzzi, S., and Charlson, R. J.: Cloud albedo enhancement by surface-active organic solutes in growing droplets, *Nature*, 401, 257-259, 10.1038/45758, 1999.
- Fanourgakis, G. S., Kanakidou, M., Nenes, A., Bauer, S. E., Bergman, T., Carslaw, K. S., Grini, A., Hamilton, D. S., Johnson, J. S., Karydis, V. A., Kirkevåg, A., Kodros, J. K., Lohmann, U., Luo, G., Makkonen, R., Matsui, H., Neubauer, D., Pierce, J. R., Schmale, J., Stier, P., Tsigaridis, K., van Noije, T., Wang, H., Watson-Parris, D., Westervelt, D. M., Yang, Y., Yoshioka, M., Daskalakis, N., Decesari, S., Gysel-Ber, M., Kalivitis, N., Liu, X., Mahowald, N. M., Myriokefalitakis, S., Schrödner, R.,  
515 Sfakianaki, M., Tsimpidi, A. P., Wu, M., and Yu, F.: Evaluation of global simulations of aerosol particle and cloud condensation nuclei number, with implications for cloud droplet formation, *Atmos. Chem. Phys.*, 19, 8591-8617, 10.5194/acp-19-8591-2019, 2019.
- Goldstein, A. H., and Galbally, I. E.: Known and Unexplored Organic Constituents in the Earth's Atmosphere, *Environmental Science & Technology*, 41, 1514-1521, 10.1021/es072476p, 2007.
- 520 Good, N., Coe, H., and McFiggans, G.: Instrumentational operation and analytical methodology for the reconciliation of aerosol water uptake under sub- and supersaturated conditions, *Atmos. Meas. Tech.*, 3, 1241-1254, 10.5194/amt-3-1241-2010, 2010a.
- Good, N., Topping, D. O., Duplissy, J., Gysel, M., Meyer, N. K., Metzger, A., Turner, S. F., Baltensperger, U., Ristovski, Z., Weingartner, E., Coe, H., and McFiggans, G.: Widening the gap between measurement and modelling of secondary organic  
525 aerosol properties?, *Atmos. Chem. Phys.*, 10, 2577-2593, 10.5194/acp-10-2577-2010, 2010b.
- Gunthe, S. S., Liu, P., Panda, U., Raj, S. S., Sharma, A., Darbyshire, E., Reyes-Villegas, E., Allan, J., Chen, Y., Wang, X., Song, S., Pöhlker, M. L., Shi, L., Wang, Y., Kommula, S. M., Liu, T., Ravikrishna, R., McFiggans, G., Mickley, L. J., Martin, S. T., Pöschl, U., Andreae, M. O., and Coe, H.: Enhanced aerosol particle growth sustained by high continental chlorine emission in India, *Nature Geoscience*, 10.1038/s41561-020-00677-x, 2021.
- 530 Gysel, M., McFiggans, G. B., and Coe, H.: Inversion of tandem differential mobility analyser (TDMA) measurements, *Journal of Aerosol Science*, 40, 134-151, <https://doi.org/10.1016/j.jaerosci.2008.07.013>, 2009.
- Hallquist, M., Wenger, J. C., Baltensperger, U., Rudich, Y., Simpson, D., Claeys, M., Dommen, J., Donahue, N. M., George, C., Goldstein, A. H., Hamilton, J. F., Herrmann, H., Hoffmann, T., Iinuma, Y., Jang, M., Jenkin, M. E., Jimenez, J. L., Kiendler-Scharr, A., Maenhaut, W., McFiggans, G., Mentel, T. F., Monod, A., Prévôt, A. S. H., Seinfeld, J. H., Surratt, J. D., Szmigielski, R., and Wildt, J.: The formation, properties and impact of secondary organic aerosol: current and emerging issues, *Atmos. Chem. Phys.*, 9, 5155-5236, 10.5194/acp-9-5155-2009, 2009.
- 535 Henry, F., Coeur-Tourneur, C., Ledoux, F., Tomas, A., and Menu, D.: Secondary organic aerosol formation from the gas phase reaction of hydroxyl radicals with m-, o- and p-cresol, *Atmospheric Environment*, 42, 3035-3045, <https://doi.org/10.1016/j.atmosenv.2007.12.043>, 2008.



- 540 Hu, D., Topping, D., and McFiggans, G.: Measured particle water uptake enhanced by co-condensing vapours, *Atmos. Chem. Phys.*, 18, 14925-14937, 10.5194/acp-18-14925-2018, 2018.
- Huff Hartz, K. E., Rosenørn, T., Ferchak, S. R., Raymond, T. M., Bilde, M., Donahue, N. M., and Pandis, S. N.: Cloud condensation nuclei activation of monoterpene and sesquiterpene secondary organic aerosol, *Journal of Geophysical Research: Atmospheres*, 110, n/a-n/a, 10.1029/2004JD005754, 2005.
- 545 Huff Hartz, K. E., Tischuk, J. E., Chan, M. N., Chan, C. K., Donahue, N. M., and Pandis, S. N.: Cloud condensation nuclei activation of limited solubility organic aerosol, *Atmospheric Environment*, 40, 605-617, <https://doi.org/10.1016/j.atmosenv.2005.09.076>, 2006.
- IUPAC: Task Group on Atmospheric Chemical Kinetic Data Evaluation, website: <http://iupac-dev.ipsl.jussieu.fr/#>.
- Jayne, J. T., Leard, D. C., Zhang, X., Davidovits, P., Smith, K. A., Kolb, C. E., and Worsnop, D. R.: Development of an Aerosol Mass Spectrometer for Size and Composition Analysis of Submicron Particles, *Aerosol Science and Technology*, 33, 49-70, 10.1080/027868200410840, 2000.
- 550 Jimenez, J. L., Jayne, J. T., Shi, Q., Kolb, C. E., Worsnop, D. R., Yourshaw, I., Seinfeld, J. H., Flagan, R. C., Zhang, X., Smith, K. A., Morris, J. W., and Davidovits, P.: Ambient aerosol sampling using the Aerodyne Aerosol Mass Spectrometer, *Journal of Geophysical Research: Atmospheres*, 108, doi:10.1029/2001JD001213, 2003.
- 555 Jimenez, J. L., Canagaratna, M. R., Donahue, N. M., Prevot, A. S. H., Zhang, Q., Kroll, J. H., DeCarlo, P. F., Allan, J. D., Coe, H., Ng, N. L., Aiken, A. C., Docherty, K. S., Ulbrich, I. M., Grieshop, A. P., Robinson, A. L., Duplissy, J., Smith, J. D., Wilson, K. R., Lanz, V. A., Hueglin, C., Sun, Y. L., Tian, J., Laaksonen, A., Raatikainen, T., Rautiainen, J., Vaattovaara, P., Ehn, M., Kulmala, M., Tomlinson, J. M., Collins, D. R., Cubison, M. J., Dunlea, J., Huffman, J. A., Onasch, T. B., Alfarra, M. R., Williams, P. I., Bower, K., Kondo, Y., Schneider, J., Drewnick, F., Borrmann, S., Weimer, S., Demerjian, K., Salcedo, D., Cottrell, L., Griffin, R., Takami, A., Miyoshi, T., Hatakeyama, S., Shimono, A., Sun, J. Y., Zhang, Y. M., Dzepina, K., Kimmel, J. R., Sueper, D., Jayne, J. T., Herndon, S. C., Trimborn, A. M., Williams, L. R., Wood, E. C., Middlebrook, A. M., Kolb, C. E., Baltensperger, U., and Worsnop, D. R.: Evolution of Organic Aerosols in the Atmosphere, *Science*, 326, 1525-1529, 10.1126/science.1180353, 2009.
- 560 Kanakidou, M., Seinfeld, J. H., Pandis, S. N., Barnes, I., Dentener, F. J., Facchini, M. C., Van Dingenen, R., Ervens, B., Nenes, A., Nielsen, C. J., Swietlicki, E., Putaud, J. P., Balkanski, Y., Fuzzi, S., Horth, J., Moortgat, G. K., Winterhalter, R., Myhre, C. E. L., Tsigaridis, K., Vignati, E., Stephanou, E. G., and Wilson, J.: Organic aerosol and global climate modelling: a review, *Atmos. Chem. Phys.*, 5, 1053-1123, 10.5194/acp-5-1053-2005, 2005.
- King, S. M., Rosenørn, T., Shilling, J. E., Chen, Q., and Martin, S. T.: Increased cloud activation potential of secondary organic aerosol for atmospheric mass loadings, *Atmos. Chem. Phys.*, 9, 2959-2971, 10.5194/acp-9-2959-2009, 2009.
- 570 Köhler, H.: The Nucleus in and the Growth of Hygroscopic Droplets., *Transactions of the Faraday Society*, 32, 1152-1161, 1936.
- Kreidenweis, S., and Asa-Awuku, A.: Aerosol Hygroscopicity: Particle Water Content and Its Role in Atmospheric Processes, 331-361 pp., 2014.



- 575 Kulmala, M., Laaksonen, A., Korhonen, P., Vesala, T., Ahonen, T., and Barrett, J. C.: The effect of atmospheric nitric acid vapor on cloud condensation nucleus activation, *Journal of Geophysical Research: Atmospheres*, 98, 22949-22958, 10.1029/93JD02070, 1993.
- 580 Lambe, A. T., Onasch, T. B., Massoli, P., Croasdale, D. R., Wright, J. P., Ahern, A. T., Williams, L. R., Worsnop, D. R., Brune, W. H., and Davidovits, P.: Laboratory studies of the chemical composition and cloud condensation nuclei (CCN) activity of secondary organic aerosol (SOA) and oxidized primary organic aerosol (OPOA), *Atmos. Chem. Phys.*, 11, 8913-8928, 10.5194/acp-11-8913-2011, 2011.
- Liu, P., Song, M., Zhao, T., Gunthe, S. S., Ham, S., He, Y., Qin, Y. M., Gong, Z., Amorim, J. C., Bertram, A. K., and Martin, S. T.: Resolving the mechanisms of hygroscopic growth and cloud condensation nuclei activity for organic particulate matter, *Nature Communications*, 9, 4076, 10.1038/s41467-018-06622-2, 2018.
- 585 Lohmann, U., and Feichter, J.: Global indirect aerosol effects: a review, *Atmos. Chem. Phys.*, 5, 715-737, 10.5194/acp-5-715-2005, 2005.
- Lowe, S. J., Partridge, D. G., Davies, J. F., Wilson, K. R., Topping, D., and Riipinen, I.: Key drivers of cloud response to surface-active organics, *Nature Communications*, 10, 5214, 10.1038/s41467-019-12982-0, 2019.
- 590 Massoli, P., Lambe, A. T., Ahern, A. T., Williams, L. R., Ehn, M., Mikkilä, J., Canagaratna, M. R., Brune, W. H., Onasch, T. B., Jayne, J. T., Petäjä, T., Kulmala, M., Laaksonen, A., Kolb, C. E., Davidovits, P., and Worsnop, D. R.: Relationship between aerosol oxidation level and hygroscopic properties of laboratory generated secondary organic aerosol (SOA) particles, *Geophysical Research Letters*, 37, n/a-n/a, 10.1029/2010GL045258, 2010.
- 595 McFiggans, G., Artaxo, P., Baltensperger, U., Coe, H., Facchini, M. C., Feingold, G., Fuzzi, S., Gysel, M., Laaksonen, A., Lohmann, U., Mentel, T. F., Murphy, D. M., O'Dowd, C. D., Snider, J. R., and Weingartner, E.: The effect of physical and chemical aerosol properties on warm cloud droplet activation, *Atmos. Chem. Phys.*, 6, 2593-2649, 10.5194/acp-6-2593-2006, 2006.
- 600 McFiggans, G., Mentel, T. F., Wildt, J., Pullinen, I., Kang, S., Kleist, E., Schmitt, S., Springer, M., Tillmann, R., Wu, C., Zhao, D., Hallquist, M., Faxon, C., Le Breton, M., Hallquist, Å. M., Simpson, D., Bergström, R., Jenkin, M. E., Ehn, M., Thornton, J. A., Alfarra, M. R., Bannan, T. J., Percival, C. J., Priestley, M., Topping, D., and Kiendler-Scharr, A.: Secondary organic aerosol reduced by mixture of atmospheric vapours, *Nature*, 565, 587-593, 10.1038/s41586-018-0871-y, 2019.
- 605 Ovadnevaite, J., Zuend, A., Laaksonen, A., Sanchez, K. J., Roberts, G., Ceburnis, D., Decesari, S., Rinaldi, M., Hodas, N., Facchini, M. C., Seinfeld, J. H., and O' Dowd, C.: Surface tension prevails over solute effect in organic-influenced cloud droplet activation, *Nature*, 546, 637, 10.1038/nature22806  
<https://www.nature.com/articles/nature22806#supplementary-information>, 2017.
- Petters, M. D., and Kreidenweis, S. M.: A single parameter representation of hygroscopic growth and cloud condensation nucleus activity, *Atmos. Chem. Phys.*, 7, 1961-1971, 10.5194/acp-7-1961-2007, 2007.
- Petters, M. D., Wex, H., Carrico, C. M., Hallbauer, E., Massling, A., McMeeking, G. R., Poulain, L., Wu, Z., Kreidenweis, S. M., and Stratmann, F.: Towards closing the gap between hygroscopic growth and activation for secondary organic aerosol – Part 2: Theoretical approaches, *Atmos. Chem. Phys.*, 9, 3999-4009, 10.5194/acp-9-3999-2009, 2009.



- 610 Petters, S. S., Pagonis, D., Claflin, M. S., Levin, E. J. T., Petters, M. D., Ziemann, P. J., and Kreidenweis, S. M.: Hygroscopicity of Organic Compounds as a Function of Carbon Chain Length and Carboxyl, Hydroperoxy, and Carbonyl Functional Groups, *The Journal of Physical Chemistry A*, 121, 5164-5174, 10.1021/acs.jpca.7b04114, 2017.
- Prenni, A. J., Petters, M. D., Kreidenweis, S. M., DeMott, P. J., and Ziemann, P. J.: Cloud droplet activation of secondary organic aerosol, *Journal of Geophysical Research: Atmospheres*, 112, 10.1029/2006JD007963, 2007.
- 615 Roberts, G. C., and Nenes, A.: A Continuous-Flow Streamwise Thermal-Gradient CCN Chamber for Atmospheric Measurements, *Aerosol Science and Technology*, 39, 206-221, 10.1080/027868290913988, 2005.
- Rudolf, R., Majerowicz, A., Kulmala, M., Vesala, T., Viisanen, Y., and Wagner, P. E.: Kinetics of particle growth in supersaturated binary vapor mixtures, *Journal of Aerosol Science*, 22, S51-S54, [https://doi.org/10.1016/S0021-8502\(05\)80032-1](https://doi.org/10.1016/S0021-8502(05)80032-1), 1991.
- 620 Ruehl, C. R., and Wilson, K. R.: Surface Organic Monolayers Control the Hygroscopic Growth of Submicrometer Particles at High Relative Humidity, *The Journal of Physical Chemistry A*, 118, 3952-3966, 10.1021/jp502844g, 2014.
- Ruehl, C. R., Davies, J. F., and Wilson, K. R.: An interfacial mechanism for cloud droplet formation on organic aerosols, *Science*, 351, 1447, 10.1126/science.aad4889, 2016.
- Seinfeld, J. H., and Pandis, S. N.: *Atmospheric chemistry and physics : from air pollution to climate change*, Third edition. ed., edited by: Pandis, S. N., John Wiley & Sons, Hoboken, New Jersey, 2016.
- 625 Shao, Y., Wang, Y., Du, M., Voliotis, A., Alfarra, M. R., Turner, S. F., and McFiggans, G.: Characterisation of the Manchester Aerosol Chamber facility, *Atmos. Meas. Tech. Discuss.*, 2021, 1-50, 10.5194/amt-2021-147, 2021.
- Shrivastava, M., Cappa, C. D., Fan, J., Goldstein, A. H., Guenther, A. B., Jimenez, J. L., Kuang, C., Laskin, A., Martin, S. T., Ng, N. L., Petaja, T., Pierce, J. R., Rasch, P. J., Roldin, P., Seinfeld, J. H., Shilling, J., Smith, J. N., Thornton, J. A., Volkamer, R., Wang, J., Worsnop, D. R., Zaveri, R. A., Zelenyuk, A., and Zhang, Q.: Recent advances in understanding secondary organic aerosol: Implications for global climate forcing, *Reviews of Geophysics*, 55, 509-559, 10.1002/2016RG000540, 2017.
- 630 Shulman, M. L., Jacobson, M. C., Carlson, R. J., Synovec, R. E., and Young, T. E.: Dissolution behavior and surface tension effects of organic compounds in nucleating cloud droplets, *Geophysical Research Letters*, 23, 277-280, <https://doi.org/10.1029/95GL03810>, 1996.
- Sun, J., and Ariya, P. A.: Atmospheric organic and bio-aerosols as cloud condensation nuclei (CCN): A review, *Atmospheric Environment*, 40, 795-820, <https://doi.org/10.1016/j.atmosenv.2005.05.052>, 2006.
- 635 Topping, D., Connolly, P., and McFiggans, G.: Cloud droplet number enhanced by co-condensation of organic vapours, *Nature Geosci*, 6, 443-446, 10.1038/ngeo1809  
<http://www.nature.com/ngeo/journal/v6/n6/abs/ngeo1809.html#supplementary-information>, 2013a.
- 640 Topping, D., Connolly, P., and McFiggans, G.: Cloud droplet number enhanced by co-condensation of organic vapours, *Nature Geoscience*, 6, 443, 10.1038/ngeo1809





<https://www.nature.com/articles/ngeo1809#supplementary-information>, 2013b.

Topping, D., Barley, M., Bane, M. K., Higham, N., Aumont, B., Dingle, N., and McFiggans, G.: UManSysProp v1.0: an online and open-source facility for molecular property prediction and atmospheric aerosol calculations, *Geosci. Model Dev.*, 9, 899-914, 10.5194/gmd-9-899-2016, 2016.

645 VanReken, T. M., Ng, N. L., Flagan, R. C., and Seinfeld, J. H.: Cloud condensation nucleus activation properties of biogenic secondary organic aerosol, *Journal of Geophysical Research: Atmospheres*, 110, 10.1029/2004JD005465, 2005.

Varutbangkul, V., Brechtel, F. J., Bahreini, R., Ng, N. L., Keywood, M. D., Kroll, J. H., Flagan, R. C., Seinfeld, J. H., Lee, A., and Goldstein, A. H.: Hygroscopicity of secondary organic aerosols formed by oxidation of cycloalkenes, monoterpenes, sesquiterpenes, and related compounds, *Atmos. Chem. Phys.*, 6, 2367-2388, 10.5194/acp-6-2367-2006, 2006.

650 Wang, Y., Chen, Y., Wu, Z., Shang, D., Bian, Y., Du, Z., Schmitt, S. H., Su, R., Gkatzelis, G. I., Schlag, P., Hohaus, T., Voliotis, A., Lu, K., Zeng, L., Zhao, C., Alfarra, R., McFiggans, G., Wiedensohler, A., Kiendler-Scharr, A., Zhang, Y., and Hu, M.: Mutual promotion effect between aerosol particle liquid water and nitrate formation lead to severe nitrate-dominated particulate matter pollution and low visibility, *Atmos. Chem. Phys. Discuss.*, 2019, 1-35, 10.5194/acp-2019-716, 2019.

655 Wang, Y., Voliotis, A., Shao, Y., Zong, T., Meng, X., Du, M., Hu, D., Chen, Y., Wu, Z., Alfarra, M. R., and McFiggans, G.: Secondary organic aerosol phase behaviour in chamber photo-oxidation of mixed precursors, *Atmos. Chem. Phys. Discuss.*, 2021, 1-25, 10.5194/acp-2021-105, 2021.

Wex, H., Petters, M. D., Carrico, C. M., Hallbauer, E., Massling, A., McMeeking, G. R., Poulain, L., Wu, Z., Kreidenweis, S. M., and Stratmann, F.: Towards closing the gap between hygroscopic growth and activation for secondary organic aerosol: Part 1 – Evidence from measurements, *Atmos. Chem. Phys.*, 9, 3987-3997, 10.5194/acp-9-3987-2009, 2009.

660 Zhang, Q., Jimenez, J. L., Canagaratna, M. R., Allan, J. D., Coe, H., Ulbrich, I., Alfarra, M. R., Takami, A., Middlebrook, A. M., Sun, Y. L., Dzepina, K., Dunlea, E., Docherty, K., DeCarlo, P. F., Salcedo, D., Onasch, T., Jayne, J. T., Miyoshi, T., Shimojo, A., Hatakeyama, S., Takegawa, N., Kondo, Y., Schneider, J., Drewnick, F., Borrmann, S., Weimer, S., Demerjian, K., Williams, P., Bower, K., Bahreini, R., Cottrell, L., Griffin, R. J., Rautiainen, J., Sun, J. Y., Zhang, Y. M., and Worsnop, D. R.: Ubiquity and dominance of oxygenated species in organic aerosols in anthropogenically-influenced Northern Hemisphere midlatitudes, *Geophysical Research Letters*, 34, 10.1029/2007gl029979, 2007.

665 Zhao, D. F., Buchholz, A., Kortner, B., Schlag, P., Rubach, F., Fuchs, H., Kiendler-Scharr, A., Tillmann, R., Wahner, A., Watne, Å. K., Hallquist, M., Flores, J. M., Rudich, Y., Kristensen, K., Hansen, A. M. K., Glasius, M., Kourtchev, I., Kalberer, M., and Mentel, T. F.: Cloud condensation nuclei activity, droplet growth kinetics, and hygroscopicity of biogenic and anthropogenic secondary organic aerosol (SOA), *Atmos. Chem. Phys.*, 16, 1105–1121, 2016.

670

675



680

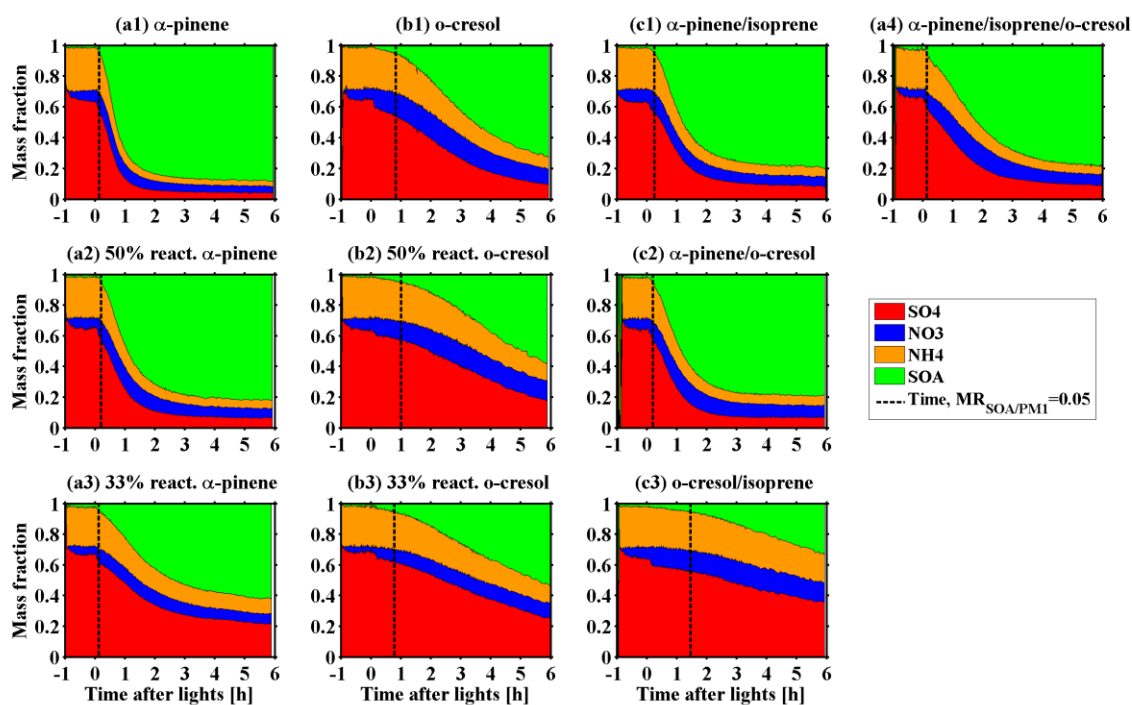


Figure 1. Mass fraction of chemical species in non-refractory  $PM_1$  measured by HR-ToF-AMS during SOA formation evolution in various VOC systems.

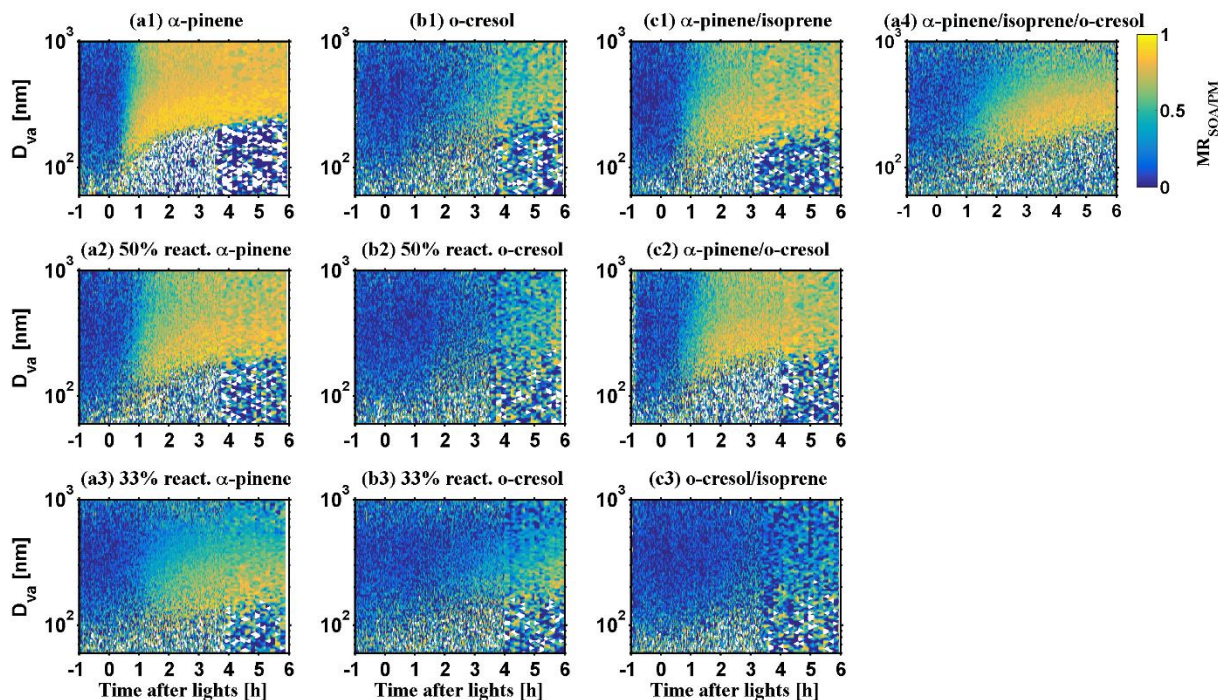


Figure 2. Size-resolved SOA mass fraction in non-refractory  $PM_{10}$  ( $MR_{SOA/PM1}$ ) measured by HR-ToF-AMS during SOA formation evolution in various VOC systems.

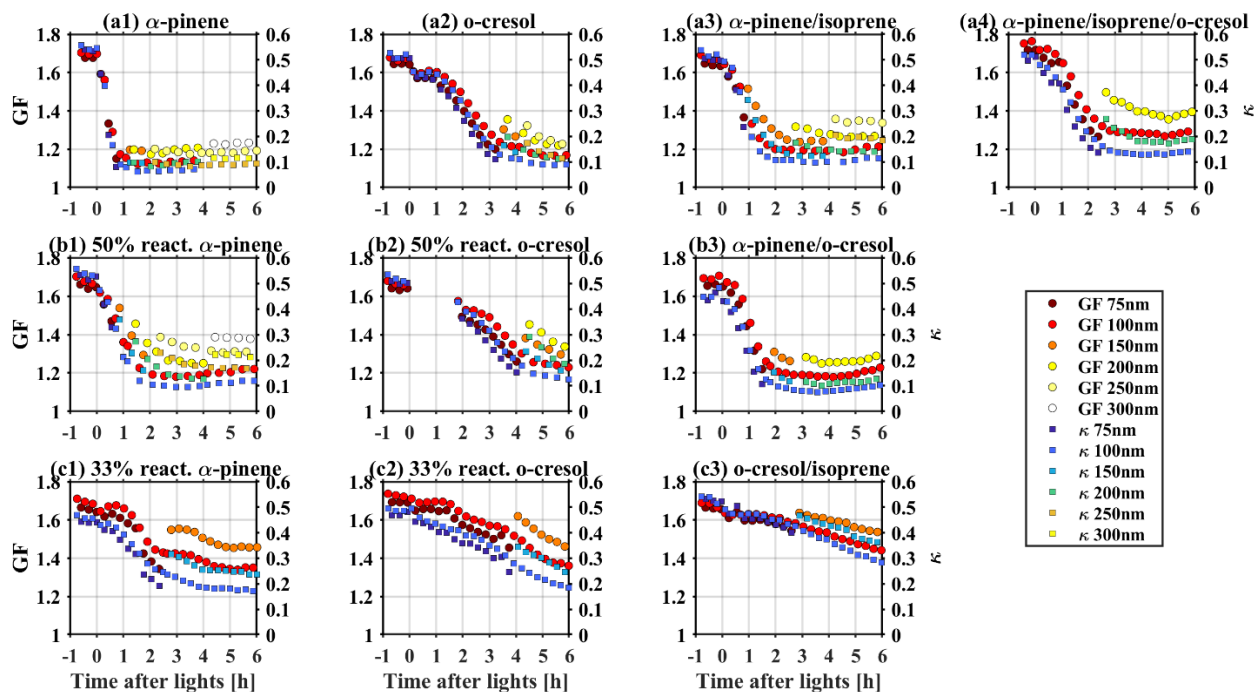


Figure 3. Time series of GF and  $\kappa$  at different measured particle size during SOA formation evolution in various VOC systems.

690

695

700

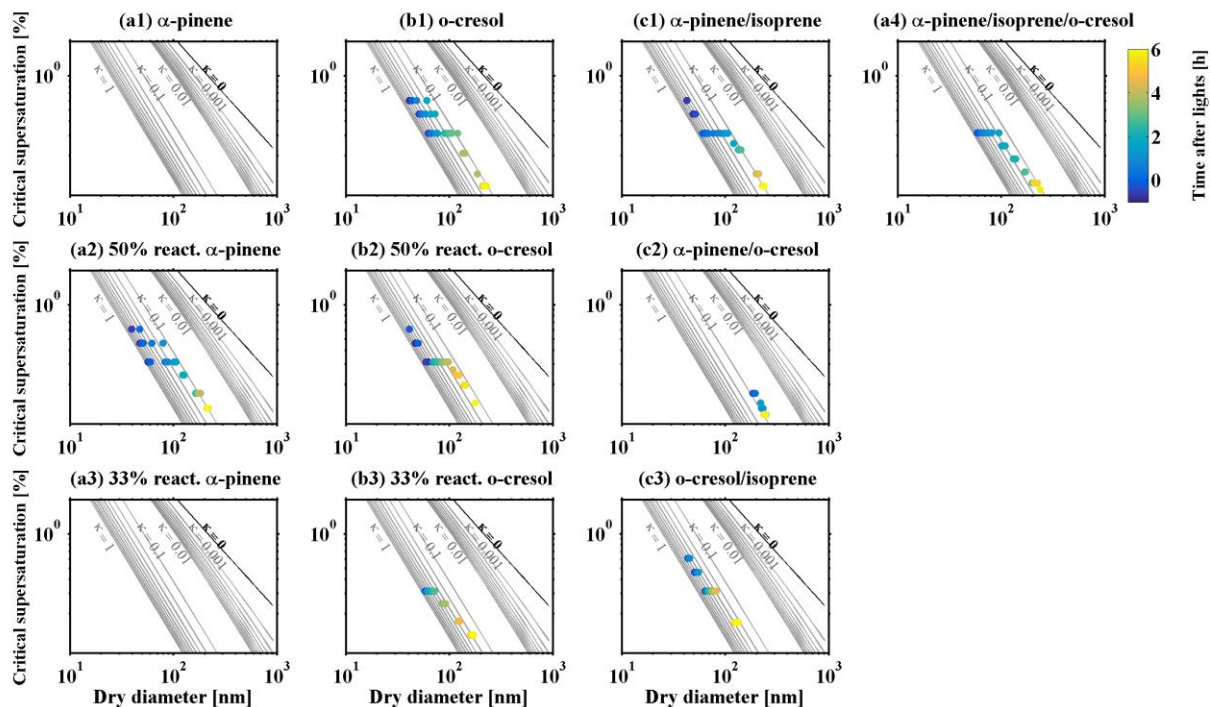


Figure 4. Critical supersaturation as a function of dry particle size ( $D_{50}$ ) measured by CCN counter during SOA formation evolution in various VOC systems. Contour lines represent hygroscopicity  $\kappa$ , calculated by following the method in Petters and Kreidenweis (2007).

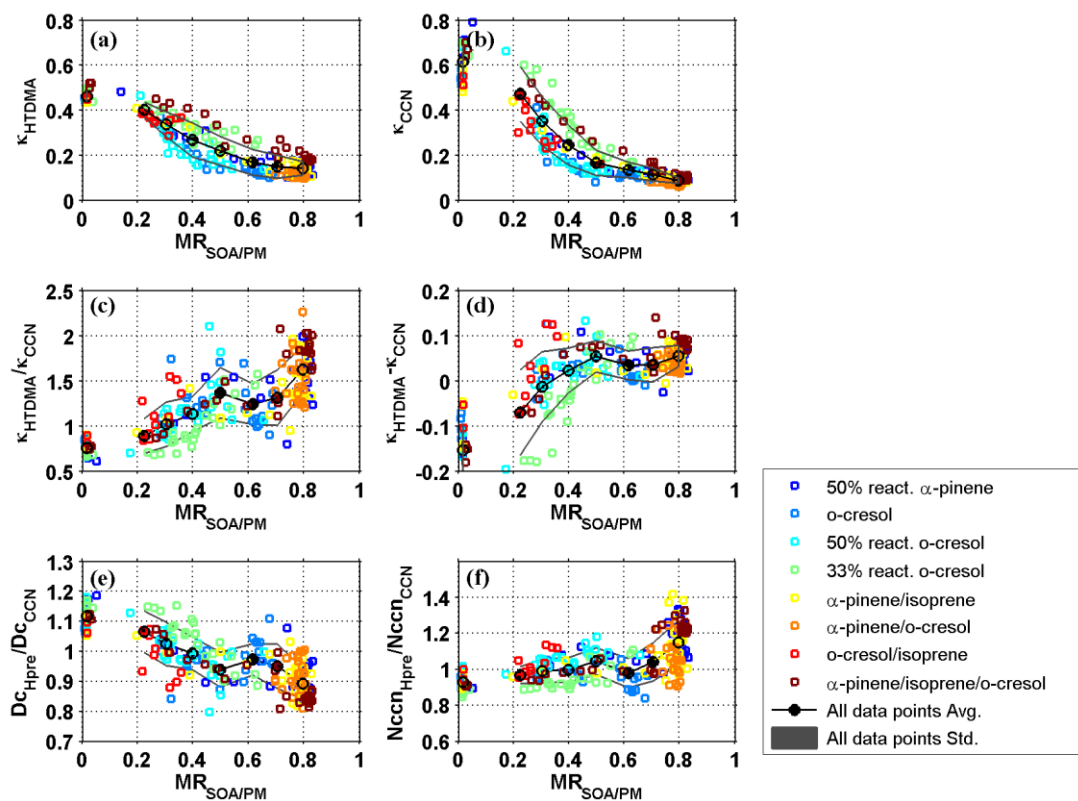


Figure 5. (a)  $\kappa_{HTDMA}$ , (b)  $\kappa_{CCN}$ , (c)  $\kappa_{HTDMA} / \kappa_{CCN}$ , (d)  $\kappa_{HTDMA} - \kappa_{CCN}$ , (e-f) critical diameter and CCN number concentration between HTDMA prediction using  $\kappa$ -Köhler theory and CCN measurement, as a function of  $MR_{SOA/PM}$  in various investigated VOC systems.